euspen's 23rd International Conference & Exhibition, Copenhagen, DK, June 2023
www.euspen.eu

Development of magnet array movable planar magnetic levitation stage

Motohiro Takahashi[1]

[1]*Research and Development Group, Hitachi, Ltd.*

motohiro.takahashi.fd@hitachi.com

Abstract
In recent years, the miniaturization of semiconductors has led to demand for nanometer-scale positioning in their manufacturing equipment. In such systems, positioning errors are mainly caused by friction, heat deformation, and strain from the roller guide. In addition, throughput is mainly limited by heat deformation of the stage caused by heat generation from motor coil and roller guide friction. A magnetic levitation (maglev) guide can prevent these two effects, which limit positioning accuracy, because it can realize noncontact support of the table. In particular, compared with stacked magnetic levitation stages, the moving mass is dramatically small in the maglev planar stage, enabling high speed moving with high positioning accuracy.

Furthermore, from the viewpoint of heat generation reduction in moving units, it is desirable to install magnets on the floating side and coils on the fixed side. However, the moving magnet-type planar stage should use a coil switching control system.

In this study, a new maglev planar stage system with a movable magnet array and coil switching control system was prototyped and evaluated. The basic characteristics of the prototyped maglev planar stage system were evaluated. As a result, stable levitation positioning movement by coil switching control was confirmed.

Keywords: Ultra-precision, Positioning, Magnetic bearing, Mechatronics, Stage system

1. Introduction

Eliminating the effects of friction is essential to achieve nanometer scale positioning accuracy. Therefore, various magnetic levitation (maglev) mechanisms and stages have been developed to prevent the effects of friction[1-5].

These include stages with a long stroke on a single axis [1,2], a coarse-fine stage [3,4], and a planar stage with a magnet array and coil array[5-8]. In particular, the planar-type stage has a small moving mass in both directions of the two orthogonal axes on the horizontal plane and can move in long strokes on the order of mm. However, when the magnet array is used as the stator and the coils as the mover, the large upward leakage magnetic field that occurs may limit the applicable applications. In the case of fixed coils, leakage fields from the coil array are also an issue.

The target of this research is to realize a low magnetic-field planar type magnetic levitation stage with coils as the fixed side and magnets as the movable side. The magnet array is composed of square magnets of the same size laid out to make the leakage magnetic field uniform on the table top surface.

In this report, a prototype of a movable magnet-type planar magnetic levitation stage with a current switching control function for coil arrays was prototyped, and its basic characteristics were evaluated.

2. Concept

Figure 1 shows the concept of the planar magnetic levitation stage. The levitation table can move in long strokes on both X and Y axes, and the structure of the levitation part is simple, enabling the mass of the moving part to be reduced in both X and Y axes. Lightening the weight of the moving part is advantageous for higher speeds by reducing the heat generated by the stage motor, suppressing vibration disturbance in the equipment chassis during acceleration and deceleration, and reducing the thermal load of the reaction force offsetting system.

Generally, planar magnetic levitation stages have a configuration in which the magnets are laid on a base on the fixed side and coils is placed on the levitation table side. However, in the coil-movable, magnet-fixed system, the application is limited by the leakage magnetic field generated by the magnet laid on the base. Another disadvantage is the need to run water-cooling pipes for coil cooling in two orthogonal axes.

This led to the development of a planar magnetic levitation stage with a fixed coil and movable magnets that has a small leakage magnetic field. One of the technical issues in this case is the need for coil switching control, since the levitation table with the magnet array on the bottom moves over the coil tiles laid over the entire stroke area. If the stroke is long, an amplifier with a connection switching function to the coil should be used.

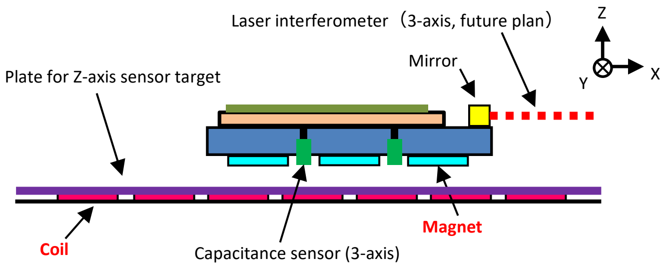

Figure 1. Concept of magnet array movable planar maglev stage

3. Structure

Figure 2 shows the configuration of the prototype planar magnetic levitation stage.

On the base side (the non-floating side), a square coil with a side of 100 mm (hereinafter referred to as "coil tile") is laid. Coil tiles are water cooled on the underside. On the floating table side, neodymium magnets are laid to form a magnet array.

To verify the concept, a prototype stage with a long stroke in X-axis direction and a small stroke in the Y-axis direction was evaluated. A linear scale is used to measure the X-direction position, since long strokes are required. In addition, two capacitance sensors for Y-direction measurement are used to measure the Y-direction position and rotation around the Z-axis. Furthermore, three Z-direction capacitance sensors are used to measure the Z-direction position and rotation around the X and Y axes.

This position measurement information is input to the controller, which calculates the thrust distribution and then performs feedback control of the amount of current in each coil tile.

Figure 3 shows a diagram of only the planar motor part. The red side of the magnet represents the N-pole and the blue side represents the S-pole. Considering the magnet area surrounded by green lines as a single unit, the configuration is similar to that of a typical three-phase AC linear motor as shown in the XZ section at the bottom of Fig. 3. In addition, unlike general linear motors, there is no opposing yoke and the magnetic flux has an X-directional component, so thrust in the vertical direction can also be obtained. When the table position changes, the positional relationship between the magnets and coils shifts and the direction and magnitude of the thrust force changes.

Table 1 shows the design specifications of the planar magnetic levitation stage to be developed. In this report, the mass of the movable table is set to 2 kg and the maximum acceleration to 9.8 m/s^2 due to the limitations of the motor dimensions.

Table 1 Design specifications of planar maglev stage

Levitation mass		2.0 kg
Dimensions		450×450×80 mm
Strokes	XY	200 mm
	Z	±3 mm
Max. Acc.		9.8 m/s^2
Sampling frequency		5 kHz
Resonance frequency		>400 Hz
Bandwidth		200 Hz

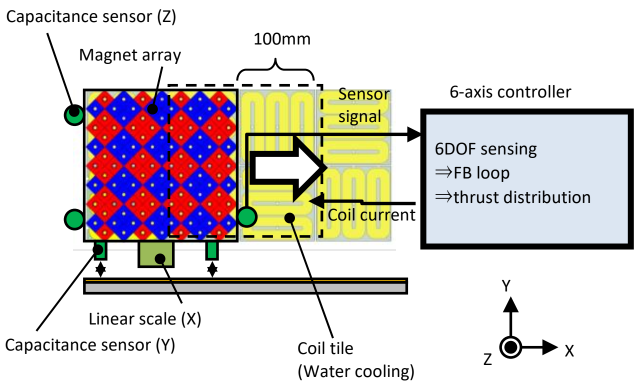

Figure 2. Configuration of prototype planar stage

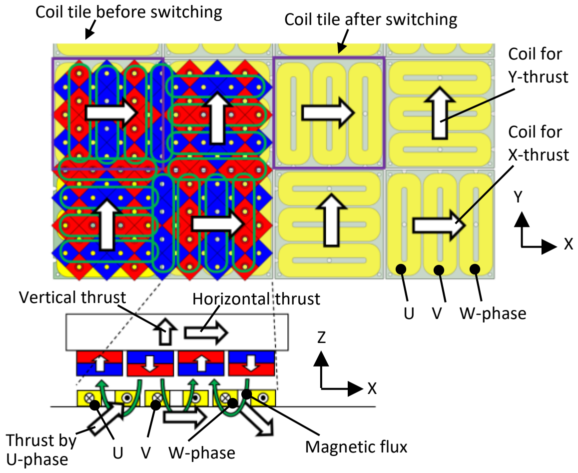

Figure 3. Configuration of planar motor

A magnetic field analysis is performed to calculate the maximum thrust. This determines the mass of the table that can be levitated. From there, the dimensions of the magnets, which account for the majority of the table mass, are limited. The same calculations are repeated until the magnet satisfies the levitatable mass constraint.

Next, the details of the magnetic field analysis of the planar motor are explained. The analysis conditions are shown in Fig. 4(a), where 3A, the rated current of the coil and amplifier, is applied to each phase of the UVW of the coil. In the case of the positional relationship between the coil and magnet as shown in Fig. 4(b), each coil generates a thrust force in the direction of the arrow in the figure (see Table 2 for detailed values). Thus, the thrust forces on each coil can be calculated and summed to obtain the horizontal and vertical partial forces produced by a single coil tile.

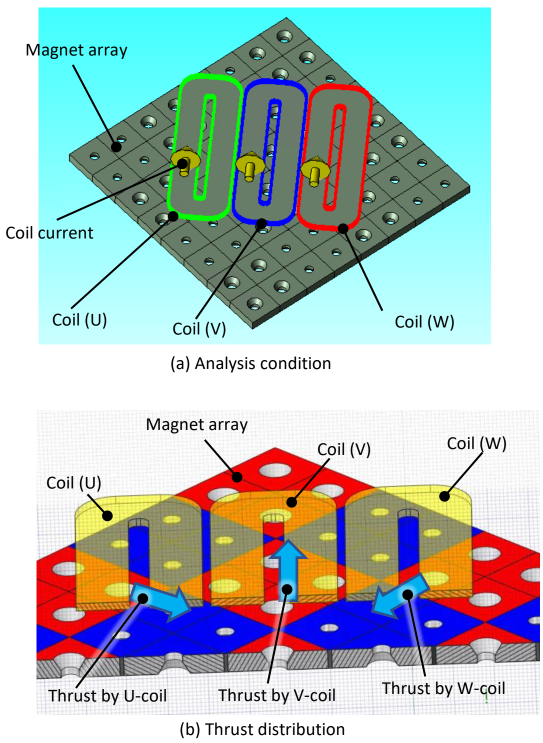

Figure 4. Condition of magnetic analysis

Figure 5 shows the vector diagram of the magnetic flux obtained from the magnetic field analysis, and Table 2 shows the horizontal and vertical thrust for each coil. These are the thrust forces when the rated current of the amplifier, 3A, is applied to each coil. For example, in the positional relationship between the coils and magnets shown in Fig.4, the horizontal thrust of phase V becomes almost zero, and only the vertical component remains. If currents in the same direction are applied to the U and W phases, their horizontal thrusts are cancelled each other. Thus, by setting the appropriate ratio of currents in each phase, the desired horizontal and vertical thrust can be obtained.

A similar analysis was performed by shifting the positional relationship between the magnets and coils, and the thrust force of each coil during table movement was analyzed. The relationship between the stage coordinates and coil currents obtained from this analysis is explained in the next section.

From this analysis, it was confirmed that the thrust in the Z direction at the rated current is 33.7 N for the total of the four coil tiles under the levitation table, which is sufficient to support the 2 kg mass of the table. In addition, two coil tiles contribute to the horizontal acceleration and deceleration. The maximum thrust at the maximum current of 6 A is 28 N and the maximum acceleration is 14 m/s^2, which meets or exceeds the design specification of 9.8 m/s^2.

Figure 6 shows a CAD model of the evaluation device to which the designed planar motor is applied.

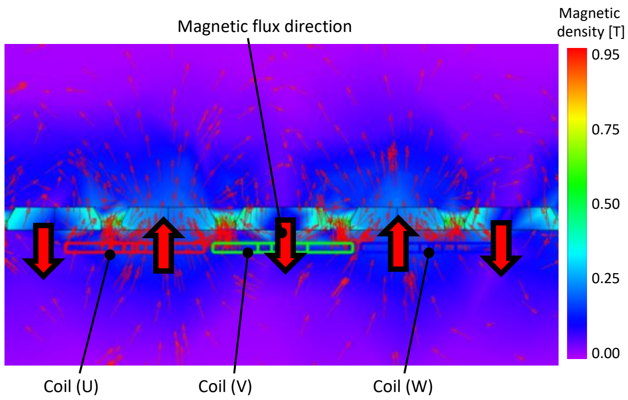

Figure 5. Analysis result of magnetic circuit

Table 2 Magnetic field analysis results

Phase	U	V	W
Horizontal thrust [N]	3.50	-0.06	-3.47
Vertical thrust [N]	-1.57	5.18	-1.68

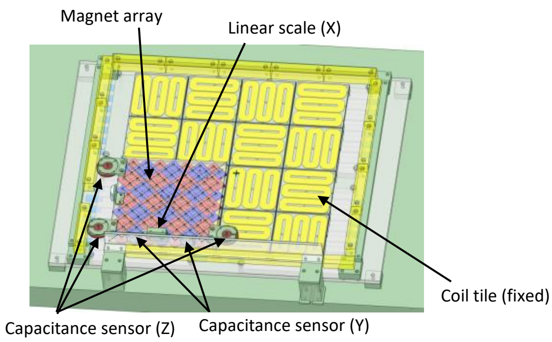

Figure 6. CAD model of prototyped maglev planar stage

4. Controller design

Figure 7 shows the controller configuration. First, the 6-DOF (6-degree-of-freedom) position and altitude are calculated from the 6ch displacement sensors. Next, they are input to the 6-axis parallel PID controller. This is then input to the position deviation of the 6-axes parallel PID controller, which can independently calculate the position and altitude by decoupling them. This calculates the thrust command values for the 6-axes and the horizontal and vertical partial forces in each coil tile to achieve them. In addition, the current values for each phase of the UVW in each coil tile are obtained.

As shown in Fig.8, when the coil tiles are numbered, consider the distribution of thrust force when the X coordinate of the levitation table changes due to stage movement. The direction of the horizontal force distribution that can be generated by each coil tile is indicated by the red arrow. A vertical directional force can be generated by all coils. Here, variables K_a to K_c, which are determined according to the X coordinate of the stage, are specified as follows.

$$K_a = {}^{x}/_{L_m} \quad \text{where} \quad 0 < K_a < 1 \tag{1}$$

$$K_b = {}^{(2x - L_m)}/_{L_m} \quad \text{where} \quad -1 < K_b < 1 \tag{2}$$

$$K_c = {}^{(L_m - x)}/_{L_m} \quad \text{where} \quad 0 < K_c < 1 \tag{3}$$

Let x be the X coordinate of the stage and L_m be the pitch of the coil tiles.

The horizontal partial force (H) and vertical partial force (V) of each coil tile can be calculated from the balance of the combined thrust force and moment of each coil tile with respect to the centre of gravity of the floating table by the following matrix calculation.

$$\begin{bmatrix} H_1 & V_1 \\ H_2 & V_2 \\ H_3 & V_3 \\ H_4 & V_4 \\ H_5 & V_5 \\ H_6 & V_6 \end{bmatrix} = \begin{bmatrix} {}^{K_c}/_2 & 0 & {}^{K_c}/_4 & {}^{K_c}/_2 & {}^{K_c}/_2 & {}^{K_c}/_2 \\ 0 & {}^{1}/_2 & {}^{1}/_4 & {}^{1}/_2 & {}^{K_c}/_2 & {}^{K_b}/_2 \\ {}^{K_a}/_2 & 0 & 0 & 0 & 0 & {}^{K_a}/_2 \\ 0 & {}^{K_c}/_2 & {}^{K_c}/_2 & -{}^{K_c}/_2 & {}^{K_c}/_2 & -{}^{K_c}/_2 \\ {}^{1}/_2 & 0 & {}^{1}/_4 & -{}^{1}/_2 & -{}^{K_b}/_2 & -{}^{K_b}/_2 \\ 0 & 0 & {}^{K_a}/_4 & {}^{K_a}/_2 & -{}^{K_a}/_2 & {}^{K_a}/_2 \end{bmatrix} \cdot \begin{bmatrix} X_Q & 0 \\ Y_Q & 0 \\ 0 & Z_Q \\ 0 & Rx_Q \\ 0 & Ry_Q \\ Rz_Q & 0 \end{bmatrix} \tag{4}$$

Furthermore, the current values (I_U to I_W) for each phase of the coil are calculated using the following equations based on the relationship between the position of the coil and magnet and the direction of the thrust force, as confirmed in the magnetic field analysis of the planar motor in the previous section.

For example, the current value of the first coil tile in Fig. 8 is expressed as follows

$$I_{U1} = H_1 \sin({}^{2\pi x}/_{L_m} + {}^{2\pi}/_3) + V_1 \cos({}^{2\pi x}/_{L_m} + {}^{2\pi}/_3) \tag{5}$$

$$I_{V1} = H_1 \sin({}^{2\pi x}/_{L_m}) + V_1 \cos({}^{2\pi x}/_{L_m}) \tag{6}$$

$$I_{W1} = H_1 \sin({}^{2\pi x}/_{L_m} - {}^{2\pi}/_3) + V_1 \cos({}^{2\pi x}/_{L_m} - {}^{2\pi}/_3) \tag{7}$$

Figure 9 shows the U-phase coil current obtained from Equation 5 as an example.

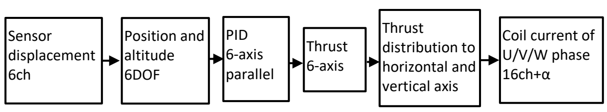

Figure 7. Configuration of controller

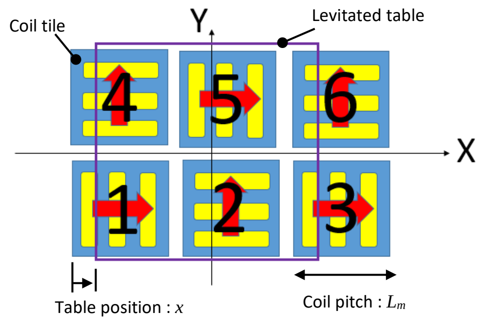

Figure 8. Pattern of fixed coil tile and parameters

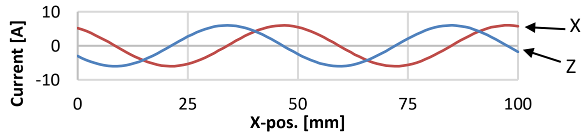

Figure 9. Coil current of U-phase for X and Z axis forces

5. Evaluation

Basic characteristics are evaluated with experimental setup shown in Fig.10. Figure 11 shows the vibration under levitation control. In the X direction, where the sensor noise is small, an amplitude of up to ±5.4 um was observed. In the Z direction, where the sensor noise was large, the vibration was also large. The proposed motor design and control system design functioned effectively, and the complex coil thrust distribution was performed with high precision to achieve a stable levitation state.

Driving characteristics during long stroke travel with coil switching were evaluated. Figure 12 shows the trajectory of a 100 mm stroke at a maximum speed of 100 mm/s and the tracking error to the target trajectory. The maximum error during the movement was 1.1 mm. The next step is to investigate whether the tracking error is due to vibration during acceleration or coil switching to further improve tracking accuracy.

6. Summary and outlook

A prototype of a planar magnetic levitation stage with a movable magnet array motor structure and coil switching control was developed and its characteristics were evaluated. Static stability for um order and mm order driving by coil switching were confirmed. However, there are still issues in nm order positioning. The roadmap to nm-order positioning is planned to further improve tracking accuracy by analysing vibration factors and introducing laser interferometry for position sensors.

References

[1] Shinshi T. A linear table system using repulsive forces of permanent magnets (Static stiffness of levitated table and its stabilization using two-axis control). *JSME*. 2001, **67**(653): 232-239.

[2] Zhou L. Trumper D. Magnetically levitated linear stage for in-vacuum transportation tasks. *In: 33 Annual conference of American Society of Precision Engineering*. 2018, 1-6.

[3] Laro D. Through the wall. *Mikroniek*. 2013, **1** 31-35.

[4] Takahashi M. Ogawa H. and Kato T. Compact maglev stage system for nanometer-scale positioning. *Precision Engineering*. 2020, **66**: 519-530.

[5] Compter I. Electro-dynamic planar motor. *Precision Engineering*. 2004, **28**: 171-180.

[6] Jansen J. et al. Magnetically levitated planar actuator with moving magnets. *IEEE Trans. on Industry Applications*. 2008, **44**(4): 1108-1115.

[7] Goos A. et al. Sensor array and algorithms for current control in a 6-DOF magnetic levitation actuator. *Proc. of the 16th Int. Conf. on New Actuators*. 2018, 1-4.

[8] Usman I. et al. Force ripple attenuation of 6-DOF direct drive permanent magnet planar levitating synchronous motors. *IEEE Trans. On Magnetics*. 2015, **51**(12): 1-8.

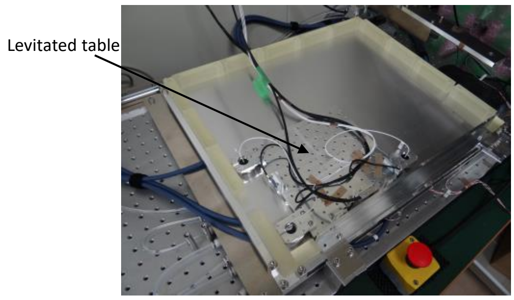

(a) Over all view

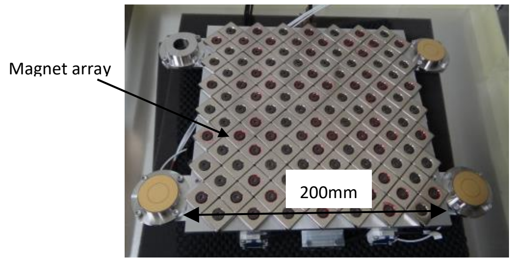

(b) Magnet array on bottom of levitated table

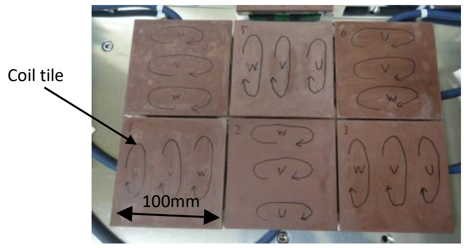

(c) Coil array on fixed base

Figure 10. Experimental setup for movable magnet planar stage

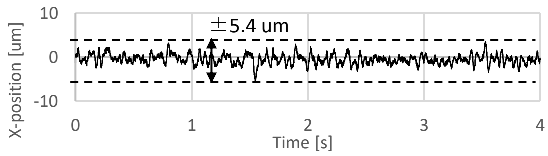

(a) X-direction

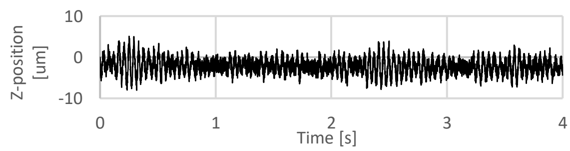

(b) Z-direction

Figure 11. Static vibration during levitation

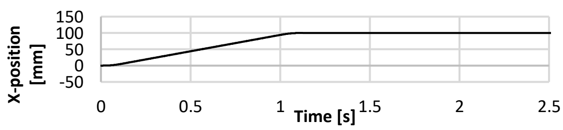

(a) Reference position

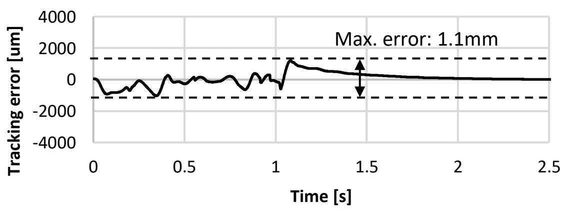

(b) Tracking error

Figure 12. Tracking error during movement